

Optical transfection using an endoscope-like system

Nan Ma,^a Frank Gunn-Moore,^b and Kishan Dholakia^a

^aUniversity of St. Andrews, School of Physics & Astronomy, St. Andrews, Fife KY16 9SS United Kingdom

^bUniversity of St. Andrews, School of Biology, Medical and Biological Sciences Building, St. Andrews, KY16 9TF United Kingdom

Abstract. Optical transfection is a powerful method for targeted delivery of therapeutic agents to biological cells. A tightly focused pulsed laser beam may transiently change the permeability of a cell membrane to facilitate the delivery of foreign genetic material into cells. We report the first realization of an endoscope-like integrated system for optical transfection. An imaging fiber (coherent optical fiber bundle) with ~ 6000 cores (pixels) embedded in a fiber cladding of $\sim 300 \mu\text{m}$ in diameter, produces an image circle (area) of $\sim 270 \mu\text{m}$ diam. This imaging fiber, with an ordered axicon lens array chemically etched at its exit face, is used for the delivery of a femtosecond laser to the cell membrane for optical transfection along with subcellular resolution imaging. A microcapillary-based microfluidic system for localized drug delivery was also combined in this miniature, flexible system. Using this novel system, a plasmid transfection efficiency up to $\sim 72\%$ was obtained for CHO-K1 cells. This endoscope-like system opens a range of exciting applications, in particular, in the targeted *in vivo* optical microsurgery area. © 2011 Society of Photo-Optical Instrumentation Engineers (SPIE). [DOI: 10.1117/1.3541781]

Keywords: optical transfection; optical injections; microendoscopes; cell surgery; coherent fiber bundles; chemical etchings.

Paper 10662 received Dec. 15, 2010; accepted for publication Dec. 16, 2010; published online Feb. 15, 2011.

1 Introduction

Laser-mediated optical nanosurgery has been developing rapidly in recent years.¹ Pulsed lasers²⁻⁴ and CW lasers⁵ spanning the infrared² to UV range of the electromagnetic spectrum⁵ have found application in this area. Two-photon microscopy,⁶ cellular microsurgery,⁷ neuron regeneration,⁸ tissue ablation,⁹ optical injection,¹⁰ and optical transfection,^{2,3} have all been widely studied. However, traditionally these forms of experiments have involved a free-space optical setup, and a high numerical-aperture objective lens, which is required to focus the laser beam onto the cellular sample. In addition, the short working distance and bulky size of microscope objectives have severely restricted the application of optical nanosurgery at deep depths. Therefore, researchers are now paying more attention to the potential use of optical fibers in order to advance such optical nanosurgery toward clinical applications. For example, Hoy et al. recently reported a miniaturized portable device for femtosecond laser microsurgery combined with two-photon imaging.¹¹ Their fiber probe had a working distance over $200 \mu\text{m}$, which could be used for deep skin treatment. In the field of optical transfection, we have recently reported an integrated optical transfection system, using a microlens-tipped single-mode optical fiber combined with a localized microfluidic gene delivery and illumination.¹² Using this setup, we achieved a transfection efficiency comparable to that obtained with traditional free-space systems. However, the necessity of an objective lens for imaging prevents this system being used for *in vivo* applications at present. On the other hand, imaging fiber-based systems with subcellular resolution have been developed¹³⁻¹⁵ and applied in tissue imaging¹⁶ and disease detection.¹⁷ Moreover, optical fiber-based Raman spectroscopy¹⁸ and fiber-based optical coherence tomography¹⁹

have all been developed. Generally, the use of optical fiber-based systems is gaining more importance in the field of biophotonics.

Here we report the first endoscope-like cell transfection system based on a commercially available imaging fiber. We simultaneously combine epifluorescence imaging with subcellular resolution, femtosecond laser light delivery, and microfluidic localized drug delivery. In order to achieve this, the exit face of an imaging fiber was chemically modified to create an ordered axicon array in order to increase the intensity and decrease the waist size ($\sim 3.75 \mu\text{m}$) of the output laser beam at a relatively remote distance ($\sim 5 \mu\text{m}$). A membrane permeable green fluorescent dye was used as a cell indicator. We successfully carried out optical transfection experiments with this system on Chinese Hamster Ovary (CHO-K1) cells. This system may be readily adapted for a number of laser mediated *in vivo* or *ex vivo* optical microsurgery experiments.

2 Experiment

2.1 Imaging Fiber Preparation

An imaging fiber (coherent optical fiber bundle) usually consists of a large number of cores (pixels), and each core can independently transmit light like a conventional single-mode optical fiber. The cores are normally laid in parallel in a honeycomb-like structure throughout the whole length (coherent configuration) of the fiber. Therefore, an image projected on to one end of the imaging fiber can be divided into pixels and transferred to the other end. The imaging fiber not only inherits most of the features of a conventional optical fiber, but it can also be used to image in traditionally unattainable environments (e.g., the stomach, intestines, bladder, lymph nodes, brain, reproductive

Address all correspondence to: Nan Ma, School of Physics & Astronomy, University of St Andrews, St. Andrews, Fife KY16 9SS United Kingdom. Tel: 44-1334-461654; Fax: 44-1334-463104; E-mail: nm210@st-andrews.ac.uk.

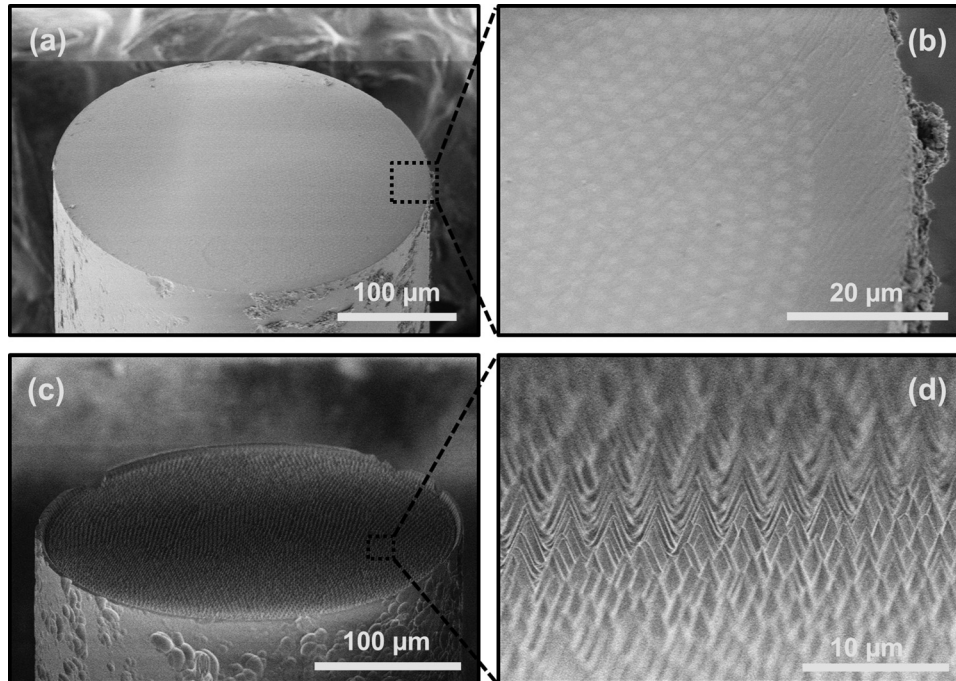


Fig. 1 (a,b) Scanning electron microscopy (SEM) image of the polished imaging fiber end face, from which (c,d) an ordered axicon array was created using a chemical etching method.

organs in females, and the prostate in men). In addition, it can substitute for an expensive articulated arm-based image acquisition setup, hence allowing its potential application into many new areas. However, the naturally divergent properties of the output beam from each core prevents imaging of objects (for example, biological cells) at a relative remote distance, which is necessary for the protection of both the fiber tip and cell from inadvertent damaging contact. Also, for optical transfection to occur, a high-intensity, micron-sized laser spot irradiated on the cell membrane is essential to initiate the required multiphoton process to permeabilize the cell membrane and minimize cell damage. Therefore a lenslike microstructure at the end face of fiber tip is needed to focus or collimate the output beams. Specifically, a microlens has to be fabricated at the tip of each core of the imaging fiber in order to achieve optical transfection and imaging simultaneously.

There are various microlensed fiber fabrication methods reported in the literature.^{12, 20–29} However, none of these procedures can readily fulfill the requirements mentioned in the previous paragraph. As such, most methods are only suitable for a conventional single-core fiber, and all of them have disadvantages such as complexity, high cost, or lack of flexibility. However, chemical etching of the polished face of imaging fiber using hydrofluoric acid (HF) can create structures at the end facet of the imaging fiber, which is favorable to our application. The etching rates of cores are slower than the cladding material of the fiber. Hence, the cores are gradually exposed to the etchant and an ordered array of conical lenses (axicon) are made from each core of the imaging fiber and are created at the end face of the imaging fiber tip.^{30–32} Each axicon can focus the output beam from each core at a relative remote position, thereby increasing the intensity of produced light and, in addition, protect both the imaging fiber tip and cells.

The imaging fiber used in this work was a commercially available product (FIGH-06-300S, Fujikura, UK), where 6000 ± 600 cores (pixels) are embedded in a fiber cladding of $300 \pm 25 \mu\text{m}$ diam, producing an image circle (area) of $270 \pm 20 \mu\text{m}$ diam. The resin coating outside of the fiber cladding was first wiped off carefully using a lens-cleaning tissue having been soaked previously in acetone for a few seconds. The conventional optical fiber cleaver and wedge-shaped diamond scribe were unable to perform a clean cleaving for our imaging fiber. Therefore, the fiber end face was manually polished using a method modified from a conventional fiber-polishing procedure.³³ A home-built holder based on a multimode fiber connector (30126G2-340, Thorlabs, UK) was used to facilitate this process. Once a flat end face was obtained [Figs. 1(a) and 1(b)], the fiber tip was chemically etched with an etchant comprising of HF (48–51%) and ammonium fluoride (NH_4F , 40%). Different mixing proportions of these two solutions can create axicons of differing angles. With a decrease in the axicon angle, transmittance from the imaging fiber decreased substantially, which can be attributed to an increase in the total internal reflection within the axicon.³⁰ On the other hand, an increase in the axicon angle will increase the diameter of the focal spot and reduce the working distance, which is detrimental to optical transfection application. In addition, because of the honeycomb-like structure and closeness of the cores, the large-angle axicon was not a preferred geometry. Therefore, a compromise volume ratio of NH_4F to HF, 1.6:1, was chosen which creates an axicon cone angle of $\sim 55^\circ$ [Figs. 1(c) and 1(d)]. The fiber tip was immersed in the etchant for 10 min at 23-deg room temperature. This procedure allows the axicon to be fully created before the cladding material was removed, thus keeping the imaging area uncompromised. The fiber tip was subsequently rinsed with both water and isopropanol, both for 30 s.

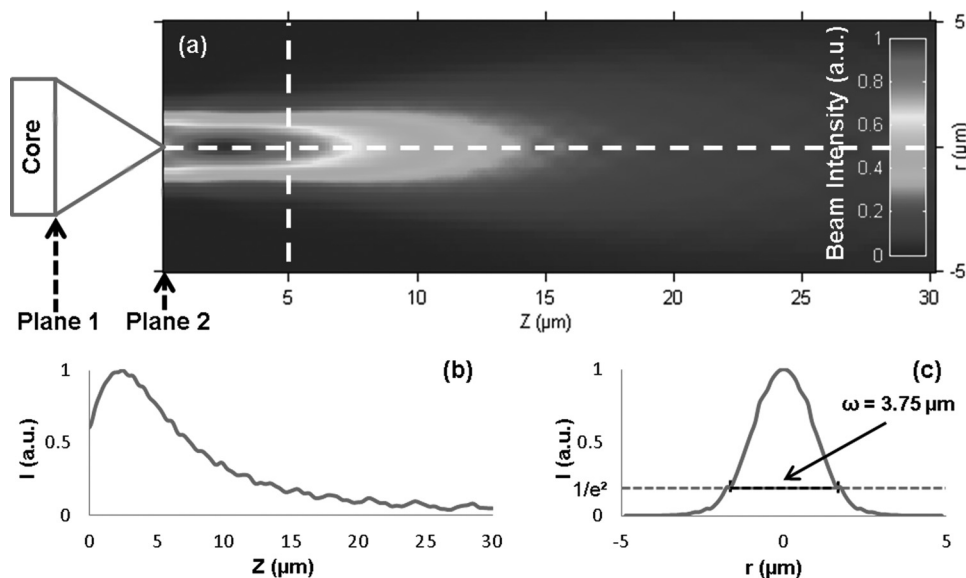


Fig. 2 (a) The simulated axial intensity profiles of the fiber output beam in water; r and Z are the cylindrical coordinates with the Z -axis pointing in the direction of the beam propagation. Planes 1 and 2 were defined at the base and apex of the axicon tip, respectively. (b) On-axis intensity distribution corresponding to the horizontal dashed line in (a). (c) Transverse intensity distribution corresponding to vertical dashed line in (a). A beam waist of $3.75 \mu\text{m}$ can be obtained from it.

2.2 Laser Output Characterization and Modeling

The imaging fiber output beam from a single core was analysed using a computer model modified from the literature,³⁴ which is proven to be precise for a wide range of different angles of the axicon tip. In the model, an axicon-tipped core was divided into a bare-tipped fiber and an axicon. The plane wave, with Gaussian intensity distribution at the end face [Fig. 2(a), plane 1] of the bare-tipped fiber, was modified by the axicon and the surrounding medium as it traveled to plane 2 [Fig. 2(a)], which was defined as the apex of the axicon perpendicular to the beam axis. The wave function at plane 2 was obtained by assigning a phase shift, calculated using geometric optics, taking into account the refractive index of the axicon and the surrounding medium to each component of the plane wave at plane 1. The light field at plane 2 was then decomposed into a spectrum of plane waves (spatial spectrum) by a Fourier transform. The spatial spectrum for any plane behind plane 2 was obtained by assigning the corresponding phase shift to each of the plane-wave components, and the light field was retrieved by an inverse Fourier transform. Using this approach, the light intensity distribution corresponding to the square of amplitude of light-field distribution can therefore be obtained. A Hankel transformation was used to reduce the calculation from 2-D to 1-D.³⁵

Figure 2(a) shows the theoretical results of the azimuthally averaged intensity profile of the beam as a function of the distance from the apex of the etched axicon in water. A $2.4\text{-}\mu\text{m}$ mode field diameter (average value from measurements) of the core, a 55-deg axicon angle and a wavelength of 800 nm were used in this modeling. The refractive index of the core and surrounding medium were assumed to be 1.5 and 1.33 , respectively. Figure 2(b) shows the on-axis intensity distribution corresponding to the horizontal dashed line in Fig. 2(a). From this can be seen that the peak intensity occurred at $\sim 2.5 \mu\text{m}$ behind the axicon apex, which was considered too short to allow safe manipulation. Therefore, cells were targeted at $5 \mu\text{m}$ away from the axicon apex during the experiment. At this distance, a

beam diameter (where the intensity falls to $1/e^2$ times the maximum value) of $3.75 \mu\text{m}$ was obtained [Fig. 2(c)]. The experimental measurements were in good agreement with theoretical predictions.

2.3 Endoscopelike System

A system for the simultaneous epifluorescence imaging and optical transection was constructed (Fig. 3). A half-wave plate was used to adjust the laser polarization direction before it was directed into a combination of a half-wave plate and an optical isolator (I-80-2, Laser2000, UK), which were then used to eliminate the backreflection from the optics. A dichroic mirror [(DM), DMLP425, Thorlabs, UK] was used to direct the incoming laser beam into the back aperture of a $10\times$ objective lens, from which the laser beam was focused onto the input end face of the imaging fiber. The coupling efficiency of the objective-imaging fiber system was $\sim 40\%$. The fiber output power was adjusted using a variable neutral density (ND) filter wheel. The fiber was mounted on an xyz translation stage (not shown in Fig. 3) and was carefully inserted into the medium. A mechanical shutter (model 845HP-02, Newport, UK) controlled the laser exposure time on the cell membrane.

For epifluorescence imaging, a fluorescence filter block (Nikon, B-2A) was used. The excitation light from $450\text{--}490 \text{ nm}$, indicated by the blue line (Fig. 3), was selected by the filter block and directed into the back aperture of the $10\times$ objective by the filter block. The output beam was subsequently focused onto the entrance face of an imaging fiber targeting at the cell sample. The fluorescence emission collected by the same beam path, indicated by the green line in Fig. 3, was imaged by a lens and CCD camera. The integrated system installed on the imaging fiber has been described previously.¹² In this work, an upgraded version of this system replaced the microlens-tipped fiber and illumination fiber from the previous setup with a single imaging fiber. Epifluorescence imaging and

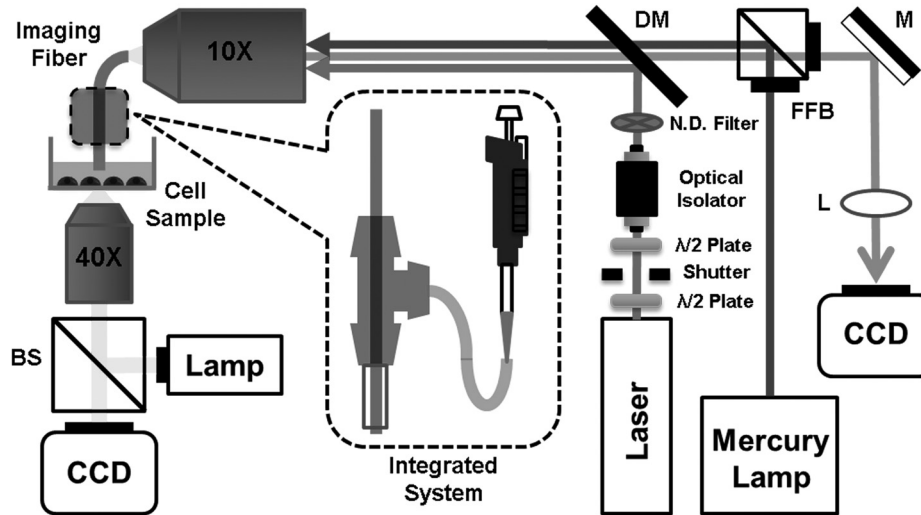


Fig. 3 Schematic of the optical path for simultaneous epifluorescence imaging and optical transfection. The femtosecond laser beam passes through two half-wave plates, a shutter, an optical isolator, and a ND filter wheel before being directed into the back aperture of the 10 × objective lens by a DM. The epifluorescence excitation emitted from mercury lamp is simultaneously directed into the back aperture of the same objective lens by a fluorescence filter block (FFB). The output beam is subsequently focused onto the entrance face of a piece of imaging fiber targeting at the cell sample. The inset shows the imaging fiber is coupled through an “integrated system” for the localized drug delivery. The fluorescence emission collected by the same beam path is imaged by a lens (L) and CCD camera. The arrows indicate the direction of the light beams. Another imaging system with illumination underneath the cell sample was used for the ease of alignment of the whole system. Notation: beam splitter (BS), mirror (M).

illumination was achieved through this imaging fiber. Another imaging system with illumination underneath the cell sample was used for the alignment of the whole system.

2.4 Cell Culture and Imaging

Chinese Hamster Ovary (CHO-K1) cells were routinely cultured in modified eagles medium (Sigma, United Kingdom) containing 10% fetal calf serum (Sera Laboratories International, UK), penicillin (100 units/ml, Sigma, UK), streptomycin (100 $\mu\text{g}/\text{ml}$, Sigma, UK), and L-Glutamine (2 mM, Sigma, UK) in a humidified atmosphere of 5% $\text{CO}_2/95\%$ air at 37°C. Cells were grown to subconfluence in 30-mm-diam glass-bottomed Petri dishes (World Precision Instruments, Stevenage, UK) in 2 ml of culturing medium. Prior to experimentation, the cell monolayer was washed twice with 2 ml of OptiMEM (Invitrogen, UK) then 2 μM of Calcein AM (Invitrogen, UK) in 1 ml of OptiMEM was added and the cells were further incubated for 15 min. The Calcein AM is a cell-membrane permeable dye. In live cells, after acetoxymethyl ester hydrolysis by intracellular esterases, the nonfluorescent Calcein AM is converted to green fluorescent calcein. The power of the beam for the fluorescent excitation (450–490 nm) of the whole imaging field was <1 mW, and the average time of exposure for each cell was <5 s. Control dishes were prepared in the same manner without the treatment by laser.

A typical image taken during experiment through the imaging fiber is shown in Fig. 4(a). Individual cores (pixels) can be clearly seen. The arrow in Fig. 4(a) indicates a cell that has been irradiated by a laser beam. Two relative brighter pixels in the center of the cell are the backreflection from the cell. However, notably the laser beam was coupled into one core of the imaging fiber, which was confirmed by the imaging system underneath cell sample (Fig. 3), and the cell was irradiated by one beam

spot at a time. According to the Nyquist-Shannon sampling theorem, the highest spatial frequencies that can be resolved are given by $1/(2d)$, where d is the core spacing in this case. Given a core spacing of $\sim 3.8 \mu\text{m}$, the lateral resolution of the current version of imaging fiber is $\sim 7.6 \mu\text{m}$, which is enough to identify individual cells. However, the contrast of the image could be enhanced through image-processing techniques. Figure 4(b) shows the processed version of Fig. 4(a) after a fast Fourier transform (FFT) bandpass filter has been applied to filter out the honeycomb-like structure and increase the intensity while subtracting background noise. A real-time image processing at 25 Hz could be realized for on-line visualization of the sample. Also by using this method, the amount of Calcein AM and the power of the excitation beam, could be reduced, therefore decreasing the amount of potential disturbance to the cells caused by the imaging.

2.5 Cell Transfection Using an Endoscopelike System

Cell transfection was achieved by using an 800-nm femtosecond Ti:sapphire laser with an output pulse duration of ~ 100 fs and a pulse repetition rate of 80 MHz (2 W average power, Coherent, MIRA). At the output end of the imaging fiber, the pulses undergo stretching mainly due to nonlinear phenomena occurring inside the fiber—self-phase modulation (SPM) and group velocity dispersion (GVD)—giving an overall pulse duration of approximately from ~ 0.8 to 1.6 ps for the imaging fiber of the length from ~ 18 to 35 cm at the laser power used during the experiment, as measured using a home-built autocorrelator.³⁶ Laser light was coupled into one core of the imaging fiber, and the output from the axicon on the other side of the imaging fiber was targeted on the cell membrane, which was located 5 μm away from the axicon apex on the center of the cell (Fig. 4). The

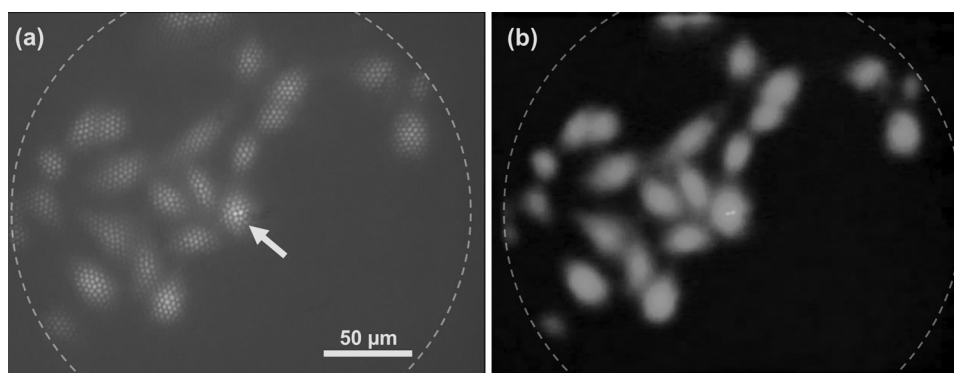


Fig. 4 (a) Fluorescent image of cells, imaged through the imaging fiber captured by the CCD camera, on the right in Fig. 3. Individual pixels can be clearly resolved. The arrow indicates a cell that is being irradiated by a laser beam. Two relatively brighter pixels in the center of the cell are the backreflection from the cell. (b) By adding a FFT bandpass filter, increasing the image intensity and then adding a background noise filter to (a), a more convenient view can be obtained. The dashed circle indicates the field of the view (image circle).

5- μm working distance is shorter when compared to the normal thickness of biological cells. Therefore, although the cell shape can be resolved, the center (peak) rather than the edge of the cell was selected for targeting by the laser. Multiple cells can be treated within one field of view by stirring the laser beam from one core to the other that sitting on top of the relative cells (Fig. 4). However, the thin layer of cladding between adjacent fiber bundle cores sometimes leads to optical cross talk in which light from neighboring image pixels (cores) can leak into one another, reducing the beam power and creating multiple spots on cell membrane.¹⁵ Thus, the consistency of the transfection would be affected; therefore, during the whole experiment the laser beam was kept within one core to ensure only one laser spot was targeted on the cell membrane at a time. Targeting different cells was achieved by either moving the imaging fiber or cell sample dish using an *xyz* translation stage. In the future, computer-assisted cell tracking³⁷ and raster-scanning techniques³⁸ may be adapted to increase the cell selectivity and transfection throughput. During our experiment, the average power of the beam was 30–70 mW. Each cell was irradiated with 3–5 laser doses. About 20 cells from each sample dish were treated in <15 min. The duration of each dose was experimentally decided to be ~ 70 ms.

The genetic material to be transfected consisted of a 1-ml solution of OptiMEM containing 20 $\mu\text{g}/\text{ml}$ mitoDsRED plasmid [encoding a mitochondrially targeted *Discoideum sp.* red fluorescent protein (BD Biosciences, Oxford, United Kingdom). This solution was delivered microfluidically through our integrated system during optical transfection.¹² After the laser treatment, the cell monolayer was washed twice with 2 ml of culturing medium before it was bathed in 2 ml of culturing medium and returned in the incubator. Then, 48 h later, the sample was viewed under a fluorescent microscope, where successfully transfected cells expressed the red fluorescent protein.

3 Results and Discussions

Transfection efficiency is defined as the number of cells correctly expressing targeted red fluorescent protein after 48 h of the laser treatment, divided by the total number of cells that were optically treated in a particular area of interest.³ In the course of this experiment, a total number of 566 CHO-K1 cells from 30 dishes were

laser treated. The transfection efficiency did not show a strong correlation with differing powers, exposure times, or pulse duration (which depends on the length of the fiber and output power). The number of spontaneously transfected cell was zero for all five control dishes. An optical transfection efficiency of up to $\sim 72\%$ and an overall 32% efficiency with this system were obtained. These transfection efficiencies compare favorably with traditional free-space microscope-based transfection³ and previous fiber-based optical transfection techniques.¹² However, a few dishes showed poorer results. This may be due to the difficulty in manipulating the short working distance ($\sim 5 \mu\text{m}$) imaging fiber. Even though a highly stabilized setup was used, a cell or a fiber end may still get damaged, resulting in a reduced transfection efficiency. To minimize this damage, during an experiment, once a potential contact between the fiber and a cell was observed, further treatment of that particular sample dish was abandoned. Also in such cases, the imaging fiber was re-etched to create an ordered axicon array at the end face before further experiments. Another factor that may affect transfection efficiency is that, due to the short working distance, the laser may have targeted the nucleus of a cell, which would reduce the cell viability, when compared to targeting at the edge of a cell.³⁹ In addition, due to SPM and GVD the pulse duration of our laser pulses targeted on cell was affected by the length of the imaging fiber, which was varied during the experiment due to the accident damage. However, on the other hand, the fluorescent imaging, cell staining, and gene delivery flow did not compromise the cell viability (data not shown).

In conclusion, we have demonstrated the first endoscope-like, fiber-based optical transfection system combined with localized microfluidic drug delivery and fluorescent imaging. In order to achieve this, an imaging fiber was used for fluorescent imaging, laser delivery, and illumination. An ordered array of microaxicons was chemically created at the polished exit surface of the imaging fiber in order to increase the light intensity at a relative remote distance. This device is a step forward toward achieving an endoscopic system for *in vivo* optical transfection applications because it is possible to achieve imaging with subcellular resolution with this device. New engineering methods have to be developed to achieve an imaging fiber with a better working distance, which would enhance the reproducibility of this device. However, this new system opens up prospects for a miniaturized,

objective free probe that could greatly reduce the cost and might be applied in tissue slices or clinical *in vivo* optical transfection applications. In future, other popular tools, such as two-photon microscopy, Raman spectroscopy, microfluidic chip, etc., may also be integrated with this system to make it a versatile biophotonics tool.

Acknowledgments

We thank the UK Engineering and Physical Sciences Research Council for funding. K.D. is a Royal Society-Wolfson Merit Award holder.

References

- D. J. Stevenson, F. J. Gunn-Moore, P. A. Campbell, and K. Dholakia, "Transfection by optical injection," in *The Handbook of Photonics for Medical Science*, V. V. Tuchin, Eds., pp. 87–117, CRC Press, Taylor & Francis Group, London (2010).
- U. K. Tirlapur and K. König, "Cell biology—targeted transfection by femtosecond laser," *Nature* **418**(6895), 290–291 (2002).
- D. Stevenson, B. Agate, X. Tsampoula, P. Fischer, C. T. A. Brown, W. Sibbett, A. Riches, F. Gunn-Moore, and K. Dholakia, "Femtosecond optical transfection of cells: viability and efficiency," *Opt. Express* **14**(16), 7125–7133 (2006).
- V. Venugopalan, A. Guerra, K. Nahen, and A. Vogel, "Role of Laser-Induced Plasma Formation in Pulsed Cellular Microsurgery and Micromanipulation," *Phys. Rev. Lett.* **88**(7), 078103 (2002).
- M. L. Torres-Mapa, L. Angus, M. Ploschner, K. Dholakia, and F. J. Gunn-Moore, "Transient transfection of mammalian cells using a violet diode laser," *J. Biomed. Opt.* **15**(4), 041506 (2010).
- W. Denk, J. H. Strickler, and W. W. Webb, "2-photon laser scanning fluorescence microscopy," *Science* **248**(4951), 73–76 (1990).
- N. Shen, D. Datta, C. B. Schaffer, P. LeDuc, D. E. Ingber, and E. Mazur, "Ablation of cytoskeletal filaments and mitochondria in live cells using a femtosecond laser nanoscissor," *Mech. Chem. Biosyst.* **2**(1), 17–25 (2005).
- M. F. Yanik, H. Cinar, H. N. Cinar, A. D. Chisholm, Y. S. Jin, and A. Ben-Yakar, "Neurosurgery—functional regeneration after laser axotomy," *Nature* **432**(7019), 822 (2004).
- A. A. Oraevsky, L. B. DaSilva, A. M. Rubenchik, M. D. Feit, M. E. Glinsky, M. D. Perry, B. M. Mammini, W. Small, and B. C. Stuart, "Plasma mediated ablation of biological tissues with nanosecond-to-femtosecond laser pulses: relative role of linear and non-linear absorption," *IEEE J. Sel. Top. Quantum Electron.* **2**(4), 801–809 (1996).
- J. Baumgart, W. Bintig, A. Ngezahayo, S. Willenbrock, H. M. Escobar, W. Ertmer, H. Lubatschowski, and A. Heisterkamp, "Quantified femtosecond laser based opto-perforation of living GFSHR-17 and MTH53a cells," *Opt. Express* **16**(5), 3021–3031 (2008).
- C. L. Hoy, N. J. Durr, P. Y. Chen, W. Piyawattanametha, H. Ra, O. Solgaard, and A. Ben-Yakar, "Miniaturized probe for femtosecond laser microsurgery and two-photon imaging," *Opt. Express* **16**(13), 9996–10005 (2008).
- N. Ma, P. C. Ashok, D. J. Stevenson, F. J. Gunn-Moore, and K. Dholakia, "Integrated optical transfection system using a microlens fiber combined with microfluidic gene delivery," *Biomed. Opt. Express* **1**(2), 694–705 (2010).
- W. Gobel, J. N. D. Kerr, A. Nimmerjahn, and F. Helmchen, "Miniaturized two-photon microscope based on a flexible coherent fiber bundle and a gradient-index lens objective," *Opt. Lett.* **29**(21), 2521–2523 (2004).
- C. J. Engelbrecht, F. Voigt, and F. Helmchen, "Miniaturized selective plane illumination microscopy for high-contrast *in vivo* fluorescence imaging," *Opt. Lett.* **35**(9), 1413–1415 (2010).
- B. A. Flusberg, E. D. Cocker, W. Piyawattanametha, J. C. Jung, E. L. M. Cheung, and M. J. Schnitzer, "Fiber-optic fluorescence imaging," *Nat. Methods* **2**(12), 941–950 (2005).
- T. J. Muldoon, M. C. Pierce, D. L. Nida, M. D. Williams, A. Gillenwater, and R. Richards-Kortum, "Subcellular-resolution molecular imaging within living tissue by fiber microendoscopy," *Opt. Express* **15**(25), 16413–16423 (2007).
- T. J. Muldoon, N. Thekkek, D. Roblyer, D. Maru, N. Harpaz, J. Potack, S. Anandasabapathy, and R. Richards-Kortum, "Evaluation of quantitative image analysis criteria for the high-resolution microendoscopic detection of neoplasia in Barrett's esophagus," *J. Biomed. Opt.* **15**(2), 026027 (2010).
- P. C. Ashok, G. P. Singh, K. M. Tan, and K. Dholakia, "Fiber probe based microfluidic raman spectroscopy," *Opt. Express* **18**(8), 7642–7649 (2010).
- K. M. Tan, M. Mazilu, T. H. Chow, W. M. Lee, K. Taguchi, B. K. Ng, W. Sibbett, C. S. Herrington, C. T. A. Brown, and K. Dholakia, "In-fiber common-path optical coherence tomography using a conical-tip fiber," *Opt. Express* **17**(4), 2375–2384 (2009).
- H. Y. Choi, S. Y. Ryu, J. H. Na, B. H. Lee, I. B. Sohn, Y. C. Noh, and J. M. Lee, "Single-body lensed photonic crystal fibers as side-viewing probes for optical imaging systems," *Opt. Lett.* **33**(1), 34–36 (2008).
- A. Malki, R. Bachelot, and F. Van Lauwe, "Two-step process for micro-lens-fibre fabrication using a continuous CO₂ laser source," *J. Opt. A* **3**(4), 291–295 (2001).
- Y. C. Tsai, Y. D. Liu, C. L. Cao, Y. K. Lu, and W. H. Cheng, "A new scheme of fiber end-face fabrication employing a variable torque technique," *J. Micromech. Microeng.* **18**(5), 055003 (2008).
- T. Held, S. Emonin, O. Marti, and O. Hollricher, "Method to produce high-resolution scanning near-field optical microscope probes by beveling optical fibers," *Rev. Sci. Instrum.* **71**(8), 3118–3122 (2000).
- P. N. Minh, T. Ono, Y. Haga, K. Inoue, M. Sasaki, K. Hane, and M. Esashi, "Bach fabrication of microlens at the end of optical fiber using self-photolithography and etching techniques," *Opt. Rev.* **10**(3), 150–154 (2003).
- R. Guo, S. Z. Xiao, X. M. Zhai, J. W. Li, A. D. Xia, and W. H. Huang, "Micro lens fabrication by means of femtosecond two photon photopolymerization," *Opt. Express* **14**(2), 810–816 (2006).
- J. Kim, M. Han, S. Chang, J. W. Lee, and K. Oh, "Achievement of large spot size and long collimation length using UV curable self-assembled polymer lens on a beam expanding coreless silica fiber," *IEEE Photon. Technol. Lett.* **16**(11), 2499–2501 (2004).
- H. Aouani, F. Deiss, J. Wenger, P. Ferrand, N. Sojic, and H. Rigneault, "Optical-fiber-microsphere for remote fluorescence correlation spectroscopy," *Opt. Express* **17**(21), 19085–19092 (2009).
- G. Cojoc, C. Liberale, P. Candeloro, F. Gentile, G. Das, F. De Angelis, and E. Di Fabrizio, "Optical micro-structures fabricated on top of optical fibers by means of two-photon photopolymerization," *Microelect. Eng.* **87**(5-8), 876–879 (2010).
- C. Liberale, G. Cojoc, P. Candeloro, G. Das, F. Gentile, F. De Angelis, and E. Di Fabrizio, "Micro-optics fabrication on top of optical fibers using two-photon lithography," *IEEE Photon. Technol. Lett.* **22**(7), 474–476 (2010).
- S. K. Eah, W. Jhe, and Y. Arakawa, "Nearly diffraction-limited focusing of a fiber axicon microlens," *Rev. Sci. Instrum.* **74**(11), 4969–4971 (2003).
- S. Szunerits, P. Garrigue, J. L. Bruneel, L. Servant, and N. Sojic, "Fabrication of a sub-micrometer electrode array: Electrochemical characterization and mapping of an electroactive species by confocal Raman microspectroscopy," *Electroanalysis* **15**(5-6), 548–555 (2003).
- A. Chovin, P. Garrigue, P. Vinatier, and N. Sojic, "Development of an ordered array of optoelectrochemical individually readable sensors with submicrometer dimensions: Application to remote electrochemiluminescence imaging," *Anal. Chem.* **76**(2), 357–364 (2004).
- THORLABS, "Guide to connectorization and polishing optical fibers," THORLABS (2006).
- T. Cizmar, "Optical traps generated by non-traditional beams," PhD Thesis, p. 127, Masaryk University, Brno (2006).
- J. W. Goodman, *Introduction to Fourier Optics*, McGraw-Hill, New York (1996).

36. F. Hache, T. J. Driscoll, M. Cavallari, and G. M. Gale, "Measurement of ultrashort pulse durations by interferometric autocorrelation: Influence of various parameters," *Appl. Opt.* **35**(18), 3230–3236 (1996).
37. D. J. Carnegie, T. Cizmar, J. Baumgartl, F. J. Gunn-Moore, and K. Dholakia, "Automated laser guidance of neuronal growth cones using a spatial light modulator," *J. Biophoton.* **2**(11), 682–692 (2009).
38. M. Antkowiak, M. L. Torres-Mapa, F. Gunn-Moore, and K. Dholakia, "Application of dynamic diffractive optics for enhanced femtosecond laser based cell transfection," *J. Biophoton.* **3**(10-11), 696–705 (2010).
39. K. Kuemeyer, J. Baumgart, H. Lubatschowski, and A. Heisterkamp, "Repetition rate dependency of low-density plasma effects during femtosecond-laser-based surgery of biological tissue," *Appl. Phys. B* **97**(3), 695–699 (2009).